Chemistry Europe
European Chemical Societies Publishing

Special Collection

G4 Sensing Pyridyl-Thiazole Polyamide Represses *c-KIT* Expression in Leukemia Cells

Raj Paul,[a] Debasish Dutta,[a] Tania Das,[a] Manish Debnath,[a] and Jyotirmayee Dash*[a]

Abstract: Specific sensing and functional tuning of nucleic acid secondary structures remain less explored to date. Herein, we report a thiazole polyamide **TPW** that binds specifically to *c-KIT1* G-quadruplex (G4) with sub-micromolar affinity and ~1:1 stoichiometry and represses *c-KIT* proto-oncogene expression. **TPW** shows up to 10-fold increase in fluorescence upon binding with *c-KIT1* G4, but shows weak or no quantifiable binding to other G4s and *ds26 DNA*. **TPW** can increase the number of G4-specific antibody (BG4) foci and mark G4 structures in cancer cells. Cell-based assays reveal that **TPW** can efficiently repress *c-KIT* expression in leukemia cells via a G4-dependent process. Thus, the polyamide can serve as a promising probe for G-quadruplex recognition with the ability to specifically alter *c-KIT* oncogene expression.

Introduction

The development of small molecule ligands that selectively recognize genomic structures and modulate their stability is one of the fundamental approaches of chemical biology.[1] Besides the storage of genetic information, the regulation of gene expression is a key function of nucleic acids.[2a] Therefore, specific recognition of a gene is pivotal to selectively regulate its expression inside cells.[2b] Owing to the occurrence of G-quadruplexes (G4s) in oncogenic promoters (e.g., *c-KIT, c-MYC, BCL-2, KRAS)* and telomeres; targeting these structures has become an elegant approach for cancer therapeutics and diagnostics.[2–5] G4s adopt four-stranded stacked guanine quartets construct in the presence of monovalent cations (e.g., Na^+, K^+). The distinctive structural morphology and promising biological role make the G4s smart targets for the design of synthetic ligands.[6] Owing to globular structures of G4s with large planes, they can be targeted with high selectivity in contrary to single-stranded and duplex DNAs having linear structures.[7,8]

In the last two decades, a variety of small molecule ligands have been reported as G4 binding compounds that down-regulate mRNA and protein expression of oncogenes.[8,9] Notably, most of the reported compounds exhibit promiscuous cross reactivity and cytotoxicity; thus they might not be suitable for selective recognition and regulation of oncogenes. However, a few ligands like thiazole orange analogues, BMVC (3,6-bis(1-methyl-4-vinylpyridinium)carbazolediiodide), IMT (a benzothiazole derivative), N-TASQ have been studied to act as fluorescent light-up molecular probe for G4 detection in cancer cells.[9c] Probing quadruplex selective ligands towards cancer therapeutics and diagnostics[9c] is still a challenging objective currently. Considering the putative biological importance of quadruplexes, it is a worthy goal to develop and exploit quadruplex specific ligands as tools for potential therapies as well as to examine and understand G4-related biological mechanisms.[10,11] Herein, we delineate a potential G4 binder, which specifically recognizes quadruplex and attenuate the *c-KIT* proto-oncogene expression without influencing the morphological properties of cells.

c-KIT codifies a type-III RTK (receptor tyrosine kinase) for stem cell factor (SCF), which is a key to cell proliferation, migration, maturation and survival in different cancer types.[12] The overexpression of *c-KIT* is observed in various malignant cancers like myeloid leukemia (due to kinase mutation causing *c-KIT* protein auto phosphorylation), pancreatic cancers, Gastric Intestinal Stromal Tumors (GIST), colorectal cancers etc.[13] In particular, identification of novel antileukemic agents and markers became a challenge due to the non-adherent and drug resistance property of leukemia cells.[14] Imatinib is the only clinically approved chemotherapeutic drug which acts through preserving the bcr-abl kinase in an inert state to treat chronic myeloid leukemia (CML).[15] However, due to high mutation rate in bcr-abl kinase, imatinib resistance and its adverse effects are so common in patients with CML. Though some second generation inhibitors have been developed to circumvent the challenge, mitigating *c-KIT* oncogene expression via small molecules is considered as an effective way for the treatment of CML.[14,15] The *c-KIT* promoter comprises three neighboring regions capable of folding into parallel G4 structures: *c-KIT1*, *c-KIT** (a G-rich Sp1 binding site) and *c-KIT2* which are positioned between −109 and −182 nucleotides upstream of the ATG start site. Experimental evidence as well as theoretical studies indicate that *c-KIT1* G4 possesses parallel topology wherein one non-G-tract guanine takes part in the center of stacked G-quartets. It is noteworthy to state that the *KIT1* G4 has a strong influence on biological role of the whole promoter.[16,17] To date,

[a] *R. Paul, Dr. D. Dutta, Dr. T. Das, Dr. M. Debnath, Prof. Dr. J. Dash*
School of Chemical Sciences
Indian Association for the Cultivation of Science
Kolkata 700032 (India)
E-mail: ocjd@iacs.res.in
Homepage: http://iacs.res.in/faculty-profile.html?id=98

Supporting information for this article is available on the WWW under https://doi.org/10.1002/chem.202100907

Special Collection *This manuscript is part of an Indo-German special collection.*

it has emerged as a difficult task to develop selective inhibitors of *c-KIT*.

In this work, we have developed a G4 sensing bis-thiazole polyamide that preferentially binds to *c-KIT1* G4, and modulates *c-KIT* expression in leukemia cells (Figure 1).

Results and Discussion

We have designed and synthesized a new class of thiazole polyamide and studied the binding interactions with several G4 structures present in the proto-oncogene promoter (*c-KIT1*, *c-KIT2*, *c-MYC*, *BCL-2*, *KRAS*), telomeres *(h-TELO)* and *ds26* DNA.

G-quadruplex ligand design and synthesis

Polyamides are known to bind B-DNA[18a] and non B-DNA structures[18b] in a sequence-specific manner. Their cellular uptake can further be improved by tuning the physicochemical parameters. Several polyamides are known to recognize DNA minor grooves[18b,c] and modulate gene expression inside cells exogenously. Thiazole moiety is present in numerous natural products and pharmaceuticals that exhibit potent biological activities. Notably, the five-membered thiazole component is present in promising antitumor agents like bleomycin (induces DNA damage), dasatinib (inhibitor of Bcr-Abl tyrosine kinase), tiazofurin (IMP dehydrogenase inhibitor).[19] We have designed and synthesized thiazole ligands having pyridine/benzene core that could bind to G-tetrad via π-π stacking interactions. In addition, –NMe2 groups present in the ligand with pyridine core could impart water solubility and binding with G4s through electrostatic interactions.[20]

Bis-thiazole ligands (Figure S1, Supporting Information) were prepared in two to three steps by using easily accessible starting materials. Bis-thiazole esters **TBE** and **TPE** with a benzene and pyridine ring were synthesized by amide coupling of isophthalic acid **1** and pyridine-2,6-dicarboxylic acid **2** with thiazolyl amino ester **5** via the corresponding acid chlorides **3** and **4**. Ester hydrolysis afforded the corresponding bisacids **TBA** and **TPA** (Scheme 1). The amine side chains were subsequently incorporated by amide coupling of **TPA** with dimethylamino propylamine **6** using HBTU as a coupling reagent to obtain the compound **TPW** (Scheme 1).

These compounds contain two thiazole rings. **TPE**, **TPA** and **TPW** contain a pyridine ring and ligands **TBE** and **TBA** contain a benzene core. In polyamide **TPW**, water soluble side chains are connected with the thiazoles through amide bond formation. Thiazole polyamide **TPW**, the bis esters (**TPE** and **TBE**) and the bis acids (**TPA** and **TBA**) were studied as G4 targeting compounds for exogenous tuning of oncogene expression using different biophysical and in-cellulo assays.

TPW selectively recognizes *c-KIT1* G-quadruplex

FRET based melting assay

The G4 stabilizing ability of **TPW**, **TPE**, **TPA**, **TBE** and **TBA** was evaluated by FRET based melting assay on a panel of 5′-FAM and 3′-TAMRA tagged G4 forming sequences (*c-KIT1*, *c-KIT2*, *c-MYC (Pu27)*, *BCL-2*, *KRAS*, *VEGF*, *h-TELO*) and *ds26* DNA or *duplex*

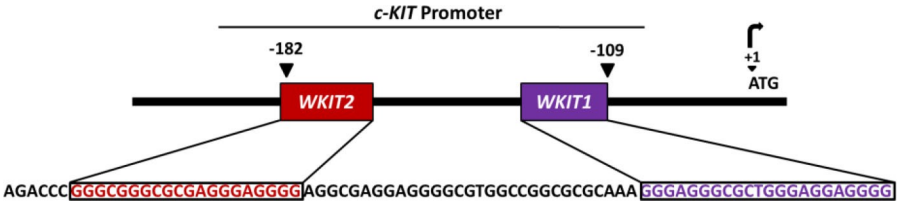

Figure 1. Schematic representation of native *c-KIT* constructs containing wild-type promoter region. *WKIT1* and *WKIT2* represent the wild type *c-KIT1* and *c-KIT2*, respectively.

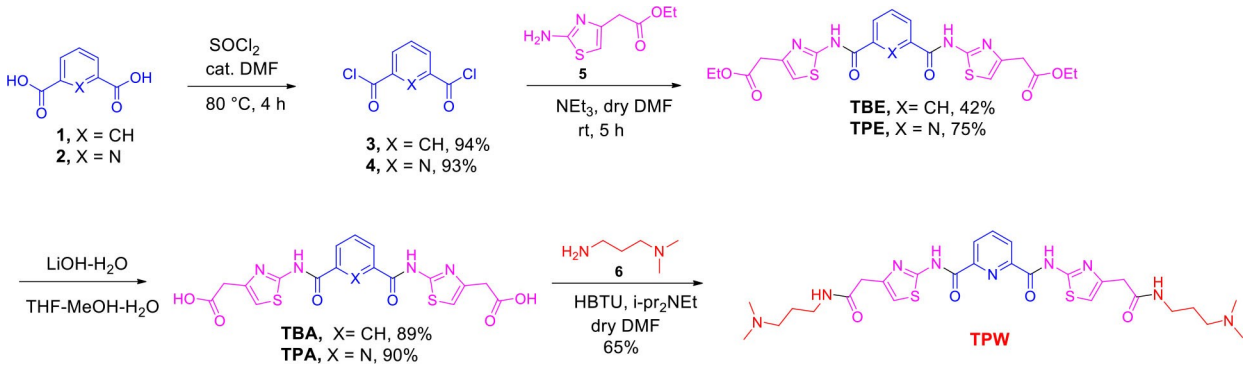

Scheme 1. Synthesis of bis-thiazole compounds containing a benzene ring and pyridine ring.

DNA. This high throughput method is used to determine the stabilization induced by the ligand for the G4s and *ds26* DNA by comparing the melting temperature (T_M) of control (without ligand) and ligand bound DNA.[21] Negligible changes in melting temperature ($\Delta T_M = 0$ to 1.4 °C) were observed for all the investigated G4s with **TPE**, **TPA**, **TBE** and **TBA** up to 10 μM (50 equivalent con.). **TPW** displayed ΔT_M values of 4.8 °C, 2.7 °C and 1.6 °C for *c-KIT1*, *c-KIT2* and *c-MYC* respectively at 1 μM concentration. Intriguingly, **TPW** did not alter the T_M of *BCL-2*, *KRAS*, *VEGF* and *h-TELO* G4s. An overall highest stabilization for *c-KIT1* G4 ($\Delta T_M = 4.8$ °C) was observed with **TPW** at 1 μM (5 equivalent con.) (Figure 2). The melting temperature of *ds26* DNA was not altered with any of these ligands. These results indicate that **TPW** selectively stabilizes *c-KIT1* G4 compared to other investigated G4s and *ds26* DNA.

A competition study by FRET was also performed to further examine the selectivity of **TPW** with *c-KIT1* G4 over *ds26* and *ct* (*calf thymus*) DNA (Figure S2, Supporting Information). The melting temperature of 200 nM 5′-FAM *c-KIT1* TAMRA −3′ was observed with **TPW** (1 μM) in the presence of 10 μM *ds26* (*ds26*:*c-KIT1* = 50:1) and *ct* DNA (*ct*:*c-KIT1* = 50:1). **TPW** did not cause any change in ΔT_M value (4.8 °C) of *c-KIT1* G4 in the presence of excess concentration of *ds26* and *ct* DNA (50 equivalent con.).

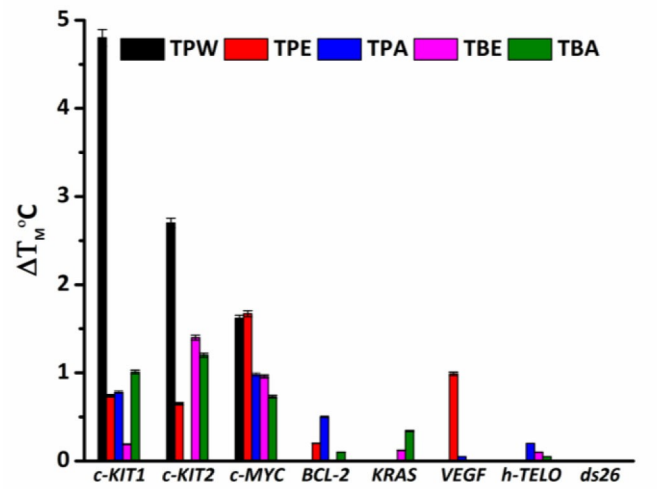

Figure 2. Thermal stabilization values (ΔT_M) of the G4s (*c-KIT1*, *c-KIT2*, *c-MYC*, *BCL-2*, *KRAS*, *VEGF*, *h-TELO*) and *ds26* DNA in presence of **TPW**, **TPE**, **TPA**, **TBE** and **TBA** at 1 μM concentration in 60 mM potassium cacodylate buffer (pH 7.4).

Fluorometric titrations

Fluorescence emission profile reveals that **TPW** exhibits a maximum at 355 nm upon excitation at 290 nm while **TPE** (λ_{ex} 325 nm) and **TPA** (λ_{ex} 290 nm) display a maxima at 455 nm. **TBE** and **TBA** exhibit a fluorescence maximum at ~440 nm when excited at 290 nm. Fluorescence emission intensity of **TPW** altered significantly upon incremental addition of pre-annealed *c-KIT1* G4 DNA (Figure 3A, Figure S3, Supporting Information). Remarkably, a new peak generated at 455 nm with a ~10-fold fluorescence enhancement (quantum yield, $\Phi = 0.094$) (Figure 3E, Table 1). Only moderate changes in fluorescence (~2 fold) were detected when **TPW** was titrated with *c-MYC* G4. However, no noticeable changes in fluorescence intensity were observed after adding sufficient concentrations (up to 5 μM) of other quadruplexes like *c-KIT2*, *KRAS*, *BCL-2*, *h-TELO* and *ds26* DNA (Figure S3, Supporting Information).

The fluorescence maxima of **TPA**, **TBE** and **TBA** were not altered significantly in the presence of *c-KIT1* and other investigated quadruplexes. The changes in fluorescence intensity were used to determine the binding affinities of ligands for quadruplexes and *ds26* DNA. **TPW** displays a dissociation constant (K_d) value of *0.44* μM (determined by Hill1 equation) for the *c-KIT1* quadruplex (Table 1, Figure 3A). The K_d value of **TPW** for *BCL-2* quadruplex and *ds26* DNA could not be determined owing to the observed insignificant changes in its fluorescence upon their addition. Moreover, the K_d values of **TPW** for *c-KIT2* (*15* μM), *c-MYC* (*12* μM), and *KRAS* (*19* μM) were determined to be higher compared to *c-KIT1* G4. This suggests that **TPW** is highly selective towards *c-KIT1* G4 over other investigated G4s and *ds26* DNA.

The fluorescence intensity of **TPE** quenched up to ~7.4 fold and ~7.1 fold in the presence of *c-KIT1* ($K_d = 0.74$ μM) and *KRAS* ($K_d = 0.97$ μM) quadruplexes, respectively while ~4.5 fold quenching was observed with *c-KIT2* ($K_d = 2.2$ μM) and *ds26* ($K_d = 2.8$ μM) (Table 1, Figure 3B, Figure S4, Supporting Information). **TPE** also displayed a K_d of *3.8* μM for *h-TELO*. These results indicate that ligand **TPE** shows non-specific binding to all the studied G4s and *ds26* sequences. Thiazole ligands **TPA**, **TBE** and **TBA** showed insignificant changes in fluorescence intensity

Table 1. Fluorescence titration study to determine binding affinity (K_d) and fold intensities (F/F_0).

DNA[a]	TPW K_d[b]	TPW F/F_0[c]	TPE K_d[b]	TPE F_0/F[c]	TPA K_d[b]	TPA F/F_0[c]	TBE K_d[b]	TBE F/F_0[c]	TBA K_d[b]	TBA F/F_0[c]
c-KIT1	*0.44*	9.87	*0.74*	7.35	*>30*	1.56	*n.d.*	1.25	*20*	1.20
c-KIT2	*15*	1.26	*2.2*	4.47	*6.7*	2.93	*n.d.*	1.52	*16*	1.22
c-MYC	*12*	2.19	*6.8*	1.84	*9*	2.81	*n.d.*	1.12	*21*	1.29
BCL-2	*n.d.*	0.94	*5.3*	1.90	*21*	1.17	*n.d.*	1.17	*23*	1.09
KRAS	*19*	1.24	*0.97*	7.13	*17*	1.39	*n.d.*	1.26	*20*	1.20
h-TELO	*n.d.*	0.98	*3.9*	3.20	*18*	1.39	*n.d.*	1.54	*19*	1.28
ds26	*n.d.*	1.2	*3*	4.41	*14*	1.50	*n.d.*	2.18	*20*	1.08

[a] The oligonucleotides were pre-annealed in 60 mM potassium cacodylate buffer (pH 7.4). [b] The binding affinity expressed in μM ($K_d = \pm 5\%$). [c] Fold change in terms of initial (F_0) and final (F) fluorescence intensity. n.d. = not determined

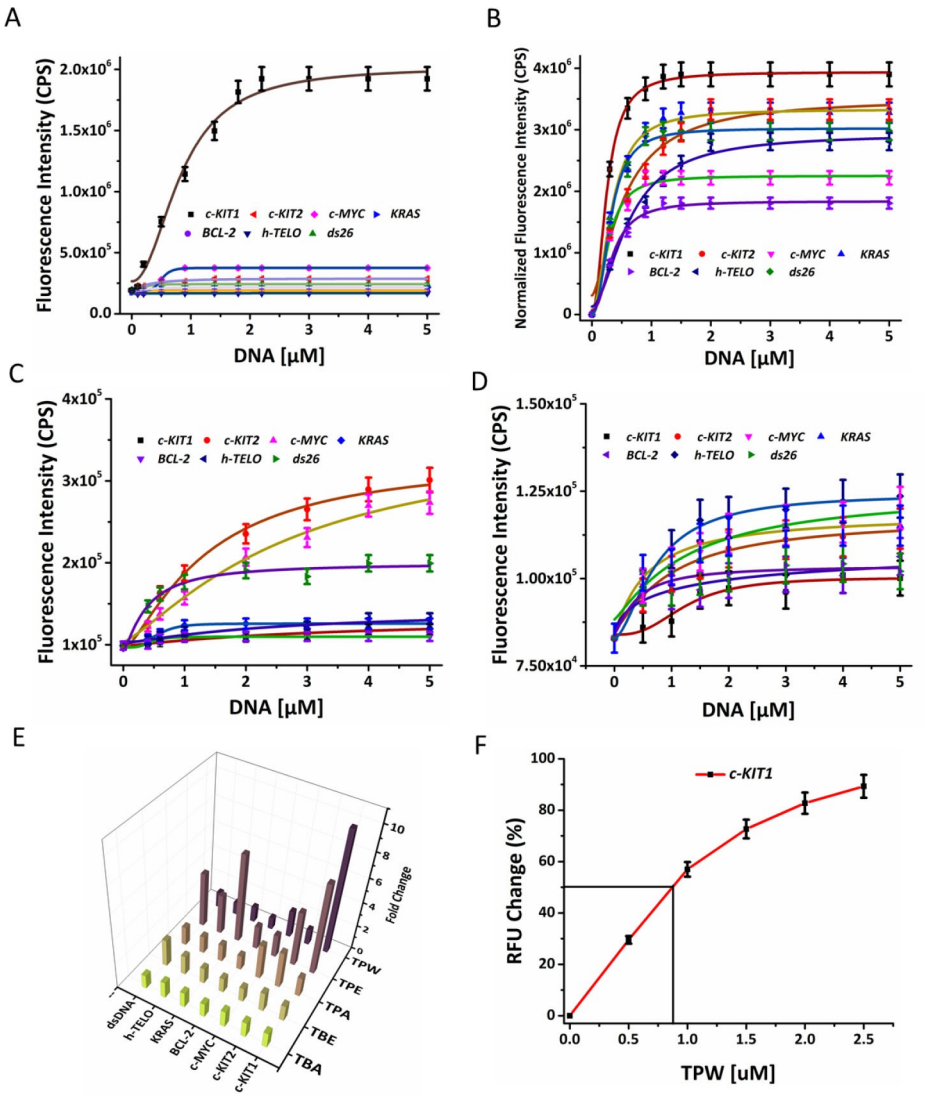

Figure 3. Fluorometric titration of (A) **TPW** (10 μM) and (B) **TPE** (10 μM), (C) **TPA** (10 μM), and (D) **TBA** (10 μM) in the presence of G4s (*c-KIT1*, *c-KIT*2, *c-MYC*, *KRAS*, *BCL-2*, *h-TELO*) and *ds26* DNA. (E) 3D Bar diagram showing fluorescence intensity fold change of **TPW**, **TPE**, **TPA**, **TBE** and **TBA** after addition of DNA up to 5 μM. (F) Thiazole orange displacement in terms of Relative Fluorescence Units (RFU) change (%) after titration of **TPW** with *c-KIT1* quadruplex.

after titration with quadruplexes and *ds26* DNA and exhibited low K_d values for quadruplexes in comparison to **TPW** and **TPE** (Table 1, Figure S5–S7, Supporting Information). The K_d values of **TBE** for the quadruplexes and *ds26* DNA could not be determined owing to negligible changes in fluorescence after addition of pre-annealed quadruplexes and *ds26* DNA. Notably, despite **TPE** displayed comparable binding affinity for *c-KIT1*, **TPW** showed far greater selectivity towards this particular quadruplex DNA. These results indicate that **TPE**, containing ester end groups can also interact with DNA sequences.

The affinity of **TPW** for the *c-KIT1* G-quadruplex was further analyzed by evaluating its ability to displace TO (thiazole-orange) from TO bound *c-KIT1* G4 (Figure 3F). **TPW** exhibited a DC_{50} value of 0.88 μM for *c-KIT1* G4. This result is in accord with the fluorescence titration data suggesting its higher affinity for the *c-KIT1* G4. However, the DC_{50} value for other G4s could not be determined due to insignificant changes in fluorescence after addition of **TPW** up to 5 μM.

Calorimetric titrations

In order to further validate the fluorescence data and obtain thermodynamic insights into the interaction of thiazole ligands with *c-KIT1* and other quadruplexes, isothermal titration calorimetry experiments were performed. These ligands differed significantly in their binding affinity towards quadruplexes and *ds26* DNA. Thermodynamic analysis revealed a typical sigmoidal binding isotherm of **TPW** for *c-KIT1* over other investigated quadruplexes and *ds26.* The binding isothermal profile was fitted using an appropriate binding site model. More importantly, the K_d value of **TPW** for *c-KIT1* determined using ITC (*0.69* μM) was in agreement with the K_d value obtained from

fluorescence titration (Table 2, Figure 4). In comparison, **TPW** possessed weak binding affinity for *c-KIT2* ($K_d = 7.4$ μM), *c-MYC* ($K_d = 29$ μM), *KRAS* ($K_d = 5.5$ μM), and *h-TELO* ($K_d = 33$ μM) (Table 2, Figure S9, Supporting Information). However, the K_d values for *BCL-2* and *ds26* DNA could not be obtained from the binding isotherms of **TPW**. Besides that, **TPW** possessed most favorable binding energy i.e., Gibbs free energy ($\Delta G = -8.40$ kcal/mol) for *c-KIT1* quadruplex, which signifies spontaneous interaction of **TPW** with *c-KIT1* and its high specificity towards *c-KIT1* over other quadruplexes and *ds26*.[22a,b] As shown in Table 2, **TPE** displayed more binding affinity towards *c-KIT1* ($K_d = 4.7$ μM) compared to other quadruplexes. Calorimetric data further revealed that **TPE** shows a binding affinity of *3.8* μM for *ds26* DNA, indicating more affinity towards *ds26* DNA and non-specific interaction for investigated quadruplexes (Table 2, Figure S10, Supporting Information). However, the other three compounds **TPA**, **TBE** and **TBA** did not exhibit any significant binding affinities and binding energy values for the investigated quadruplexes (Table 2, Figure S11–S13, Supporting Information). These results suggested that **TPW** shows superior selectivity for *c-KIT1* quadruplex with greater binding affinity compared to other quadruplexes and *ds26* DNA. ITC data also shows that **TPW** binds to the *c-KIT1* G4 with a ~1:1 stoichiometry. Moreover, the total binding enthalpy (the sum of individual enthalpic values from the fits) was negative for the interaction of this thiazole series with all the G4s and *ds26* DNA, suggesting that the entire process was enthalpically favorable.[22c]

Biophysical assays revealed that the polyamide **TPW** showed selective and potent electrostatic interactions with *c-KIT1* G4 and **TPE** exhibited non-specific interactions with the G4s and *ds26*. Consequently, both **TPW** and **TPE** were examined for cytotoxicity profile and oncogene regulatory roles in cancer cells by cell viability (XTT) assay, confocal microscopy, quantitative real time PCR (qRT-PCR), immunoblot and luciferase reporter assays.

Cytotoxic effects of TPW and TPE

We evaluated the IC_{50} values of **TPW** and **TPE** in cancer cells and normal cells (Figure S14, Supporting Information). **TPW** and **TPE** exerted IC_{50} values of ~70 μM and ~95 μM in myeloid leukemia (K562) cells after 24 hours of treatment, respectively. After longer incubation period of 72 h, **TPW** and **TPE** showed IC_{50} values of 48 μM and 63 μM in leukemia cells. They displayed >80 μM IC_{50} values for breast cancer (MCF-7) and lung carcinoma (A549) cell lines after 72 h of incubation period. Both ligands did not show inhibitory activity on normal kidney epithelial (NKE) cells up to 200 μM. Cell cycle analysis also

Table 2. Thermodynamic parameters obtained from Isothermal calorimetry (ITC) titrations. n.d. = not determined.

		c-KIT1	*c-KIT2*	*c-MYC*	*BCL-2*	*KRAS*	*h-TELO*	*ds26 DNA*
	K_d (μM)	*0.69 ± 0.03*	*7.4 ± 0.39*	*29 ± 1.4*	*n.d.*	*5.5 ± 0.28*	*33 ± 1.6*	*n.d.*
TPW	ΔG (kcal.mol^{-1})	−8.40	−7	−6.20	n.d.	−7.21	−6.11	n.d.
	N (sites)	1.01	1.59	1.8	n.d.	0.82	2.1	n.d.
	K_d (μM)	*4.2 ± 0.2*	*36 ± 1.8*	*13 ± 0.64*	*16 ± 0.8*	*15 ± 0.73*	*291 ± 14*	*3.8 ± 0.19*
TPE	ΔG (kcal.mol^{-1})	−7.34	−6.03	−4.30	−6.55	−6.60	−4.6	−7.40
	N (sites)	1.13	1.71	1.38	1.46	1.41	2.6	1.16
	K_d (μM)	*9.8 ± 0.49*	*18 ± 0.91*	*21 ± 1.06*	*12 ± 0.62*	*n.d.*	*n.d.*	*26 ± 1.31*
TPA	ΔG (kcal.mol^{-1})	−6.83	−6.47	−6.38	−6.69	n.d.	n.d.	−6.25
	N (sites)	0.96	1.31	1.33	1.17	n.d.	n.d.	1.42
	K_d (μM)	*22 ± 1.1*	*27 ± 1.3*	*35 ± 1.7*	*n.d.*	*21 ± 1*	*17 ± 0.87*	*33 ± 1.63*
TBE	ΔG (kcal.mol^{-1})	−6.34	−4.7	−6.08	n.d.	−6.38	−6.49	−6.12
	N (sites)	1.28	1.43	1.47	n.d.	1.19	1.08	1.37
	K_d (μM)	*30 ± 1.5*	*n.d.*	*17 ± 0.86*	*31 ± 1.5*	*12.0 ± 0.6*	*21 ± 1*	*n.d.*
TBA	ΔG (kcal.mol^{-1})	−6.16	n.d.	−6.50	−6.14	−6.72	−6.39	n.d.
	N (sites)	1.67	n.d.	1.53	1.76	1.44	1.54	n.d.

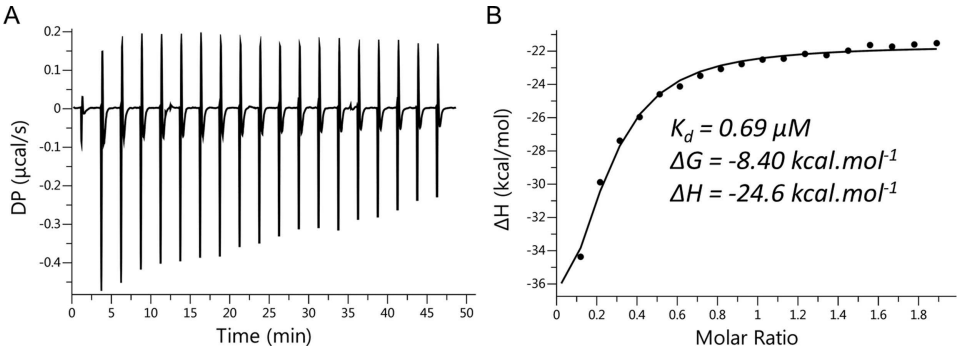

Figure 4. Representative binding isotherms for the binding of **TPW** with the *c-KIT1* G4 monitored through ITC in the presence of 60 mM potassium cacodylate buffer (pH 7.4) at 25 °C. (A) Heat burst curves and (B) the equilibrium K_d obtained through fitting the raw data.

revealed that **TPW** causes cell cycle arrest at the rate of 7% and 3.5% in S phase and G2/M phase of K562 cells respectively, at 40 μM.

TPW effectively binds to G4 DNA inside cells

Cellular localization and immunofluorescence

Confocal imaging revealed that **TPW** can efficiently enter into cancer cell nuclei and exhibit high fluorescence. It is worth noting that the fluorescence of **TPW** increased significantly inside the cellular nuclei which might be due to the interactions of **TPW** with G4s (Figure 5). Owing to the fluorescence enhancement property of **TPW** inside the cell nuclei, it can be used as a nucleus labeling probe in cancer cells.

To demonstrate whether **TPW** could enter into nucleus and bind G4s, an immunofluorescence assay (Figure 5) with BG4, a well-known G4 specific antibody was performed in HeLa cells.[23] As revealed in Figure 5, the immunofluorescence images of HeLa cells show that **TPW** efficiently entered and localized into the nucleus. The number of BG4 foci significantly increased after treatment with **TPW** as compared to untreated or control cells, indicating the ability of **TPW** to stabilize G4s at pertinent sites (Figure 5B). Confocal images further reveal that ligand **TPE** can also penetrate the cell membrane and localize into nucleus. However, **TPE** could stabilize less number of BG4 foci in comparison to **TPW**. It may be due to its non-specific interactions with DNAs and fluorescence quenching property as observed in the fluorescence experiment.

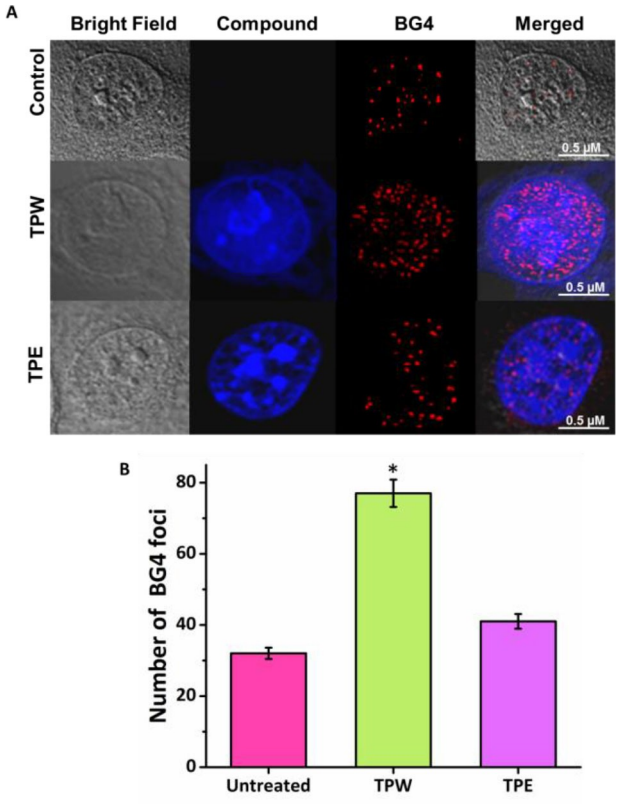

Figure 5. (A) Confocal images of HeLa cell nuclei (fixed) stained with **TPW (blue)**, **TPE (blue)** and **BG4 (red)**. (B) Quantification of BG4 foci per nucleus. For the analysis, >50 cells were counted and the standard error of the mean was calculated from three replicates. *$P < 0.05$ (Student's 't' test).

TPW preferentially represses *c-KIT* expression in K562 cells

Gene expression analysis

The gene regulatory role of both **TPW** and **TPE** on well-known G4-driven genes *c-KIT*, *c-MYC* and *BCL-2* were evaluated in K562 cells by quantifying mRNA steady-state levels using quantitative real-time PCR (Figure 6A, Figure S15, Table S1 & S2, Supporting Information). The results illustrate that **TPW** selectively represses *c-KIT* expression at m-RNA level in myeloid leukemia cells. The *c-KIT* expression level decreased significantly by 43% and 77% after treatment with **TPW** at two different doses 20 μM and 40 μM, respectively (Figure 6A). In comparison, **TPW** minimally affected the *c-MYC* and *BCL-2* expression. However, **TPE** upregulated *c-KIT* expression slightly by ~2% and ~9% at similar concentrations of 20 μM and 40 μM, respectively. Unexpectedly, **TPE** could also raise the *c-MYC* and *BCL-2* expression levels up to ~80% and 30% respectively, at 40 μM (Figure 6A).

Promoter activity assay

To investigate whether the effects of **TPW** and **TPE** on *c-KIT* expression were consequent to their binding with *KIT* promoter, the modulation on luciferase activity was studied using *c-KIT* wild promoter and pRL-TK constructs (Figure 6C). In addition, luciferase activity of *c-MYC* and *BCL-2* was also investigated to understand the specificity of ligands for a particular promoter (Figure 6C). The pRL-TK construct does not harbor G4 sequences and it is independent of G4 mediated regulation. The normalization of *c-KIT*, *c-MYC* and *BCL-2* promoter luciferase expression was accomplished with pRL-TK expression.

Apparently, **TPW** decreased the luciferase expression in a dose dependent manner for *c-KIT* promoter construct. **TPW** at two different concentrations of 20 μM and 40 μM exhibited ~25% and ~66% reduction in luciferase activity, respectively for *c-KIT* promoter, while negligible or no changes were observed for *c-MYC* and *BCL-2* expression (Figure 6B). However, **TPE** (at 40 μM concentration) increased *c-MYC* and *BCL-2* luciferase expression up to ~48% and ~40%, respectively. A mild increase in *c-KIT* expression (~10%) was also monitored at the highest dose of **TPE**. These results pointed towards the ability of **TPW** to inhibit *c-KIT* oncogene expression via its effective interactions with the promoter G-quadruplex. The observed upregulation by **TPE** might be caused due to its non-specific interaction and downstream biological effect inside the cancer cells. The detailed molecular mechanism for upregulatory effects of **TPE** will be further studied in future.

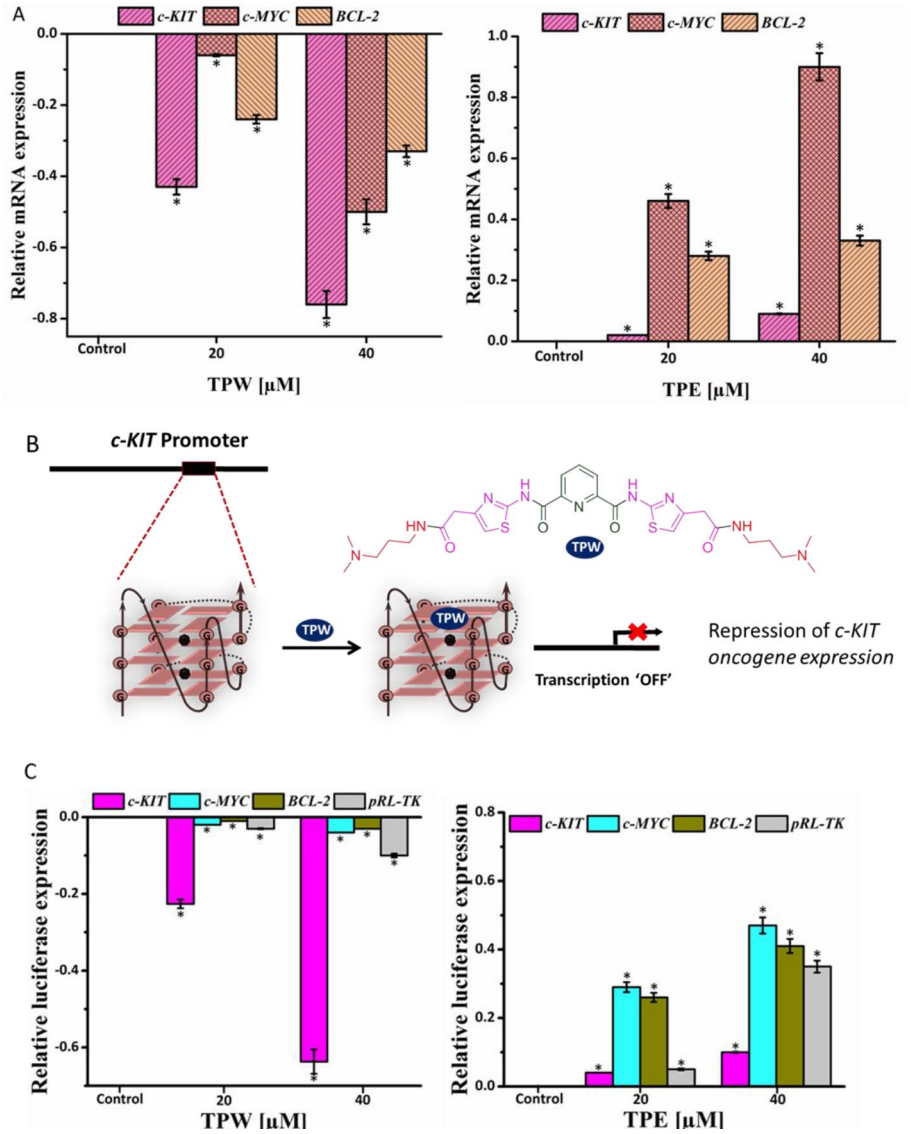

Figure 6. (A) qRT-PCR analysis for transcriptional regulation of *c-KIT*, *c-MYC* and *BCL-2* after treatment with **TPW** or **TPE** in leukemia cells (K562) for 24 h. Quantification was done in terms of fold change by double delta C_T method using 18 s rRNA or GAPDH as housekeeping or reference gene. Fold change of ligand treated relative gene expression is normalized with control or untreated value of 0. Three biological replicates were employed for the quantifications. Error bars represent mean ± SD.*$P < 0.05$ (Student's t test), versus control or untreated leukemia cells. (B) Schematic representation of **TPW** bound G4 mediated repression of *c-KIT* oncogene expression. (C) Relative luciferase expression of *c-KIT*, *c-MYC* and *BCL-2* promoters normalized with the Renilla plasmid pRL-TK after treatment with **TPW** or **TPE** at two different doses for 48 h. Fold change of ligand treated relative luciferase expression is normalized with control or untreated value of 0. Error bars correspond to mean ± SD. *$P < 0.05$ (Student's t test), versus untreated leukemia cells.

Structure-activity relationship

In order to understand the possible binding mode, docking studies of **TPW** and **TPE** were performed with *c-KIT1* (PDB: 4WO2), *c-KIT2*, *c-MYC*, *BCL-2*, *KRAS*, *h-TELO* G4s (Figure 7, Figure S19, Supporting Information). Both **TPW** and **TPE** possessed an extended conformation following energy minimization while the structures were found to adopt constrained topologies after interacting with the quadruplexes. The docking results illustrate that **TPW** can effectively stack on the 5′ end of *c-KIT1* G4 with a lowest binding energy (- 9.317 kcal.mol^{-1}) compared to other investigated G4s (Figure 7A and 7B). However, **TPE** also binds to the *c-KIT1* G4 via stacking mode of interactions but with higher energy (- 4.49 kcal.mol^{-1}) as compared to **TPW** (Figure 7C and 7D).

Modeling studies further revealed that thiazole-pyridine units of **TPW** occupy a larger plane of the G-quartet and the amine side chains participate in electrostatic interactions with the phosphate backbone. The docking results further reinforce our experimental data that thiazole incorporated molecule with water soluble amine side chains preferentially binds to *c-KIT1* G4 with 1:1 stoichiometry. Even though the G4 structures (*c-KIT1*, *c-KIT2*, *c-MYC*, *KRAS* and *BCL-2*) except *h-TELO*, employed in this work possess parallel topology, the intervening loop sequences and flanking areas (capping structures) are different. The alkyl amine-containing side chains of **TPW** play a critical

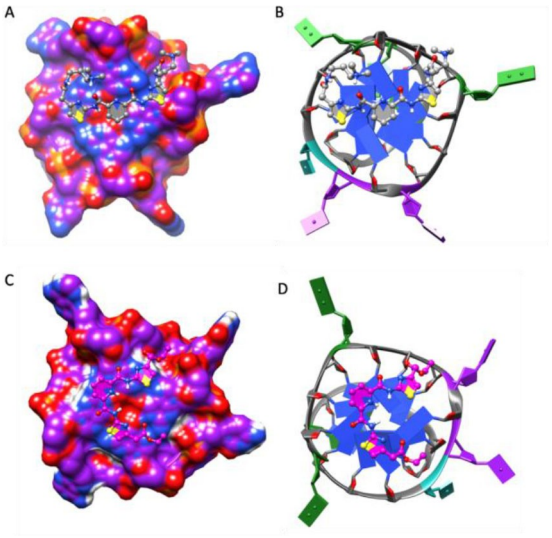

Figure 7. Molecular docking of **TPW** with *c-KIT1* (A, B) (energy = -9.317 kcal.mol^{-1}) and **TPE** with *c-KIT1* (C, D) (energy = -4.49 kcal.mol^{-1}) obtained from Autodock 4.0. Ligands (shown in stick and ball mode) stacked on a terminal G-quartet, represented as hydrophobic surface. **TPW** and **TPE** are represented in dim gray and magenta color, respectively.

role for the selective recognition of *c-KIT1* G4 (Figure 7A and 7B), due to favorable electrostatic interactions with negatively charged phosphate backbone in the groove regions of *KIT1* G4.

Conclusion

A novel and less-toxic G4 binding small molecule **TPW** selectively detects *c-KIT1* G4 and transcriptionally inhibits *c-KIT* expression in leukemia cells. This polyamide ligand containing a pyridine unit and two thiazoles preferentially targets nuclei structures and emit high fluorescence inside the cell nuclei. The expansion of such less-toxic molecules could serve as alternatives to extremely cytotoxic molecules, often used for diagnostic and therapeutic purposes. Specific targeting of genes with this class of compounds could improve bioavailability and further, their low toxicity could reduce adverse effects in cellular system. Such molecules with the potential to recognize complex biological systems could open up new avenues for the development of novel molecular agents for cancer.

Experimental Section

Synthesis of ligands: The detailed synthesis of ligands has been described in Supporting Information.

Melting experiments by FRET: The stock solution of 5′-FAM (Ex. 490 nm/Em. 520 nm) and 3′-TAMRA (Ex. 555 nm/Em. 580 nm) labeled oligo sequences were first diluted to 0.4 μM using a 60 mM potassium cacodylate (KCaco, pH 7.4) buffer. The diluted solution was then heated to 95 °C for 1 min, cooled slowly to room temperature and kept overnight at 4 °C. Subsequently, the DNA solution (0.2 μM) was incubated with the **TPW TPE TPA TBE TBA** (0 - 10 equivalent) in 60 mM potassium cacodylate buffer at pH 7.4 for 1 h, using a blank 96-well plate (Axygen) with a total volume of 100 μL for each well. In the presence of 60 mM K^+, the labeled G4 forming sequence is mainly present in a quadruplex form where the FAM is in close distance to the TAMRA showing a low FAM fluorescence due to the FRET. With increasing temperature, the conformation of G4 changes to a single-stranded form where the FAM is far from the TAMRA, which results in a high FAM fluorescence. Melting curves for the determination of melting temperature (T_M) were then obtained by recording FAM fluorescence with increasing temperatures from 37 to 95 °C at the rate of 0.9 °C/min using Roche Light Cycler II.[24] The analysis of T_M values was accomplished using OriginPro 2016 software. The ΔT_M values were then plotted against concentration of ligands to determine the stabilization potential for G4s. Further details for FRET study are provided in the Supporting Information.

Thiazole orange displacement experiment: The assay was carried out on Horiba Jobin Yvon Fluoromax 3 at room temperature in a quartz cuvette (path-length 1 mm). To perform this experiment we chose **TPW**, the most potent and selective *c-KIT1* G-quadruplex binding ligand in the series, evaluated using fluorescence titration study. DNA sequences were pre-annealed as described in fluorometric titration (Figure S13, Supporting Information). A solution of pre-annealed G4-DNA (0.25 μM) and 0.50 μM thiazole orange (TO) was prepared and incubated for 2 min and fluorescence spectrum was monitored (λ_{ex} = 501 nm; λ_{em} = 510–650 nm). Then, **TPW** was added to the solution gradually with a 2 min equilibration time, and the fluorescence was measured. The TO displacement (%) was calculated using the following basic equation:[25]

TO displacement or Relative fluorescence change (%)

$$= 100-(F/F_0 \times 100)$$

where, F denotes fluorescence intensity (F) at the emission maxima and F_0 denotes the initial fluorescence of TO–G4 complex.

The TO displacement percentage was presented as a function of concentration of mixed **TPW** to determine the DC_{50} value.

Isothermal calorimetry: Calorimetric titrations were carried out in a MicroCal PEAQ-ITC system (Malvern). The DNA samples (5 μM in 60 mM potassium cacodylate buffer, pH 7.4) were pre-annealed via heating at 95 °C for 5 min followed by gradual cooling to room temperature (0.1 °C /min) and incubated overnight at 4 °C. Experiments were performed by overfilling the pre-annealed DNA samples (5 μM) in 300 μL sample cell followed by titration with duly prepared 50 μM ligand solution over 20 injections at an interval of 150 secs. The temperature of the reference and sample cells was preserved at 25 °C during the experiment with a reference power of 10 μcal/sec and the continuous stirring of sample cell solution was maintained at a speed of 750 rpm. Samples were extensively degassed immediately before use. The raw data were analyzed by Malvern ITC Analysis software provided with the instrument. The data fitting was done using an appropriate binding model.[25b] The dissociation constant (K_d), Gibb's free energy change (ΔG), enthalpy of reaction (ΔH) and entropy (ΔS) change were calculated using the following equation:

$$\Delta G = \Delta H - T\Delta S$$

Immunodetection of G-quadruplex: Cells grown on glass cover slips were kept as control or treated with two doses of **TPW** and **TPE** (20 μM and 40 μM) for 24 h. In the following day, cells were washed with 1X PBS and fixed in chilled acetone-methanol (1:1) and permeabilized with 0.03% saponin/PBS solution. After blocking

with 3% BSA in 1X PBS, immunofluorescence was carried out using regular or standard methods, incubating at 37 °C with BG4 antibody (Mouse monoclonal, from Merck) diluted 1:200 in 1X PBS overnight, and Alexafluor 647-conjugated secondary antibody (Invitrogen) for 2 h on next day. Finally, cover slips were mounted with antified solution (Invitrogen). The BG4 emission (570–670 nm) was assembled with the excitation at 559 nm, sequentially.[26] Digital images were taken in a Confocal Laser Scanning Microscope (LSM-800, Zeiss). For the quantification of BG4 foci, >50 cells were counted using FIJI ImageJ software and the standard error of the mean was calculated from three replicates, *P <0.05 (Student's 't' test) was considered as statistically significant.

Quantitative real-time PCR (qRT PCR): K562 cells ($\sim 10^6$ per well) were placed in a 6-well plate and allowed to incubate overnight. Next day, cells were treated with **TPW** (20 μM, 40 μM) and **TPE** (20 μM, 40 μM) and harvested for 24 h. Untreated (control) cells and those treated with DMSO control were used to evaluate primary *c-KIT* expression levels. Total RNA was isolated using the TRIzol reagent (Invitrogen) according to the manufacturer's instructions. RNA quantification was carried out by a Cary Win 300 UV-Vis spectrophotometer and the total 500 ng of RNA was employed as a template for cDNA synthesis using a Verso kit (Thermo Fisher Scientific) as per the supplied protocol. Real-time PCR was carried out on Roche LightCycler 480 by the use of SYBR Premix (Applied Biosystems), according to the manufacturer's instructions. The C_T values were normalized to 18 s rRNA and compared to the untreated or control cells. The C_T method (comparative cycle threshold method) was used to calculate relative mRNA expression. The mRNA level was expressed in terms of fold changes of target gene with respect to control or untreated value of 0. Three biological replicates were employed for the quantifications. The significance level was statistically analyzed by employing a Student's t test, and results were statistically significant when *P $<$ 0.05.

Transfection and luciferase assay: K562 cells were seeded ($\sim 10^6$ cells each well) in 35 mm 6 well plates. After 16 h, cells were transiently transfected with *c-KIT*, *c-MYC* and *BCL-2* promoter (Addgene, USA) luciferase reporter construct by the use of Lipofectamine 2000 (Invitrogen), as per manufacturer's instructions. Basic empty vector pGL4.72 was employed as negative control for *c-KIT* wild promoter. pRL-TK, a HSV-thymidine kinase promoter, used as Renilla luciferase control gene (Renilla Luciferase for normalization) was employed as transfection control. After 6 h of incubation, 10% FBS was supplemented to the cells and incubated for 2 h followed by treatment with **TPW** and **TPE** at two different doses (20 μM and 40 μM). Subsequently, after 48 h of incubation, cells were lysed by 150 μl 1X cell lysis buffer (Promega) with continuous pipetting followed by vortexing for 30 secs and kept at room temperature for 10 mins. The concentration of cell lysate protein was evaluated by Lowry method.[27] The assay was performed in triplicate using Luciferase Reporter Assay System (Promega) in a Multimode microplate reader (Molecular Devices, USA). The normalization of luciferase activity was accomplished with protein concentration and the effect of ligands upon G4 constructs were normalized against the untreated or control leukemia cells.

Statistical analysis: Data were presented as the mean ± SEM and analyzed with a Student's t-tests using OriginPro 2016 software. *P* value of ≤ 0.05 indicates statistically significant.

Acknowledgements

R.P. thanks DST-India for INSPIRE Fellowship. D.D. thanks CSIR-India for a research fellowship. T.D. thanks DBT-India for a research fellowship. The authors thank Mrs. Debapriya Dutta, IACS for Confocal Microscopy. This work was supported by the Wellcome Trust/DBT India Alliance Fellowship [Grant Number, IA/S/18/2/503986] and Department of Science and Technology SwarnaJayanti Fellowship [DST/SJF/CSA-01/2015-16].

Conflict of Interest

The authors declare no conflict of interest.

Keywords: c-KIT · G-quadruplexes · leukemia · polyamide · TPW

[1] M.-H. Hu, J. Zhou, W.-H. Luo, S.-B. Chen, Z.-S. Huang, R. Wu, J.-H. Tan, *Anal. Chem.* **2019**, *91*, 2480–2487.
[2] a) S. Balasubramanian, L. H. Hurley, S. Neidle, *Nat. Rev. Drug Discovery* **2011**, *10*, 261; b) S. Mandal, Y. Kawamoto, Z. Yue, K. Hashiya, Y. Cui, T. Bando, S. Pandey, M. E. Hoque, M. A. Hossain, H. Sugiyama, *Nucleic Acids Res.* **2019**, *47*, 3295–3305.
[3] a) A. P. David, A. Pipier, F. Pascutti, A. Binolfi, J. Weiner, M. Andrea, E. Challier, S. Heckel, P. Calsou, D. Gomez, *Nucleic Acids Res.* **2019**, *47*, 7901–7913; b) M. L. Bochman, K. Paeschke, V. A. Zakian, *Nat. Rev. Genet.* **2012**, *13*, 770; c) E. Y. N. Lam, D. Beraldi, D. Tannahill, S. Balasubramanian, *Nat. Commun.* **2013**, *4*, 1796.
[4] a) K. V. Diveshkumar, S. Sakrikar, F. Rosu, S. Harikrishna, V. Gabelica, P. Pradeepkumar, *Biochemistry* **2016**, *55*, 3571–3585; b) J. Amato, L. Cerofolini, D. Brancaccio, S. Giuntini, N. Iaccarino, P. Zizza, S. Iachettini, A. Biroccio, *Nucleic Acids Res.* **2019**, *47*, 9950–9966; c) T. Frelih, B. Wang, J. Plavec, P. Šket, *Nucleic Acids Res.* **2020**, *48*, 2189–2197.
[5] S. Jonchhe, C. Ghimire, Y. Cui, S. Sasaki, M. McCool, S. Park, K. Iida, K. Nagasawa, H. Sugiyama, H. Mao, *Angew. Chem. Int. Ed.* **2019**, *58*, 877–881; *Angew. Chem.* **2019**, *131*, 887–891.
[6] a) A. I Laguerre, L. Stefan, M. Larrouy, D. Genest, J. Novotna, M. Pirrotta, D. Monchaud, *J. Am. Chem. Soc.* **2014**, *136*, 12406–12414; b) X. Wang, C.-X. Zhou, J.-W. Yan, J.-Q. Hou, S.-B. Chen, T.-M. Ou, L.-Q. Gu, Z.-S. Huang, J.-H. Tan, *ACS Med. Chem. Lett.* **2013**, *4*, 909–914.
[7] M. Zuffo, A. Guédin, E.-D. Leriche, F. Doria, V. Pirota, V. Gabelica, J.-L. Mergny, M. Freccero, *Nucleic Acids Res.* **2018**, *46*, e115–e115.
[8] S. Asamitsu, T. Bando, H. Sugiyama, *Chem. Eur. J.* **2019**, *25*, 417–430.
[9] a) A. Minard, D. Morgan, F. Raguseo, A. Di Porzio, D. Liano, A. G. Jamieson, M. Di Antonio, *Chem. Commun.* **2020**, *56*, 8940–8943; b) B. Zheng, M.-T. She, W. Long, Y.-Y. Xu, Y.-H. Zhang, X.-H. Huang, W. Liu, J.-Q. Hou, W.-L. Wong, Y.-J. Lu, *Chem. Commun.* **2020**, *56*, 15016–15019; c) P. Chilka, N. Desai, B. Datta, *Molecules* **2019**, *24*, 752.
[10] a) J. Dash, P. S. Shirude, S.-T. D. Hsu, S. Balasubramanian, *J. Am. Chem. Soc.* **2008**, *130*, 15950–15956; b) M. Nadai, F. Doria, M. Scalabrin, V. Pirota, V. Grande, G. Bergamaschi, V. Amendola, F. R. Winnerdy, A. T. n Phan, S. N. Richter, *J. Am. Chem. Soc.* **2018**, *140*, 14528–14532; c) D. Moorhouse, A. M. Santos, M. Gunaratnam, M. Moore, S. Neidle, J. E. Moses, *J. Am. Chem. Soc.* **2006**, *128*, 15972–15973.
[11] a) A. Głuszyńska, B. Juskowiak, M. Kuta-Siejkowska, M. Hoffmann, S. Haider, *Molecules* **2018**, *23*, 1134; b) S. Asamitsu, S. Obata, Z. Yu, T. Bando, H. Sugiyama, *Molecules* **2019**, *24*, 429.
[12] L. K. Ashman, R. Griffith, *Expert Opin. Invest. Drugs* **2013**, *22*, 103–115.
[13] a) M. Bejugam, M. Gunaratnam, S. Müller, D. A. Sanders, S. Sewitz, J. A. Fletcher, S. Neidle, S. Balasubramanian, *ACS Med. Chem. Lett.* **2010**, *1*, 306–310; b) D. Wei, J. Husby, S. Neidle, *Nucleic Acids Res.* **2014**, *43*, 629–644; c) K. I. McLuckie, Z. A. Waller, D. A. Sanders, D. Alves, R. Rodriguez, J. Dash, G. J. McKenzie, A. R. Venkitaraman, S. Balasubramanian, *J. Am. Chem. Soc.* **2011**, *133*, 2658–2663.
[14] a) X. Xia, Y.-C. Lo, A. A. Gholkar, S. Senese, J. Y. Ong, E. F. Velasquez, R. Damoiseaux, J. Z. Torres, *ACS Chem. Biol.* **2019**, *14*, 994–1001; b) T. Furitsu, T. Tsujimura, T. Tono, H. Ikeda, H. Kitayama, U. Koshimizu, H. Sugahara, J. H. Butterfield, L. K. Ashman, Y. Kanayama, *J. Clin. Invest.* **1993**, *92*, 1736–1744.
[15] a) E. Weisberg, P. W. Manley, S. W. Cowan-Jacob, A. Hochhaus, J. D. Griffin, *Nat. Rev. Cancer.* **2007**, *7*, 345–356; b) Q.-L. Guo, H.-F. Su, N. Wang, S.-R. Liao, Y.-T. Lu, T.-M. Ou, J.-H. Tan, D. Li, Z.-S. Huang, *Eur. J. Med. Chem.* **2017**, *130*, 458–471.

[16] a) R. Rigo, C. Sissi, *Biochemistry* **2017**, *56*, 4309–4312; b) C. Ducani, G. Bernardinelli, B. R. Högberg, B. K. Keppler, A. Terenzi, *J. Am. Chem. Soc.* **2019**, *141*, 10205–10213; c) A. T. Phan, V. Kuryavyi, S. Burge, S. Neidle, D. J. Patel, *J. Am. Chem. Soc.* **2007**, *129*, 4386–4392; d) P. S. Shirude, B. Okumus, L. Ying, T. Ha, S. Balasubramanian, *J. Am. Chem. Soc.* **2007**, *129*, 7484–7485.
[17] a) Z. A. Waller, S. A. Sewitz, S.-T. D. Hsu, S. Balasubramanian, *J. Am. Chem. Soc.* **2009**, *131*, 12628–12633; b) A. Chauhan, S. Paladhi, M. Debnath, S. Mandal, R. N. Das, S. Bhowmik, J. Dash, *Bioorg. Med. Chem.* **2014**, *22*, 4422–4429; c) S. Rankin, A. P. Reszka, J. Huppert, M. Zloh, G. N. Parkinson, A. K. Todd, S. Ladame, S. Balasubramanian, S. Neidle, *J. Am. Chem. Soc.* **2005**, *127*, 10584–10589.
[18] a) G. Padroni, J. A. Parkinson, K. R. Fox, G. A. Burley, *Nucleic Acids Res.* **2018**, *46*, 42–53; b) M. J. Cocco, L. Hanakahi, M. D. Huber, N. Maizels, *Nucleic Acids Res.* **2003**, *31*, 2944–2951; c) M. A. Marques, R. M. Doss, S. Foister, P. B. Dervan, *J. Am. Chem. Soc.* **2004**, *126*, 10339–10349.
[19] a) D. Dutta, M. Debnath, D. Müller, R. Paul, T. Das, I. Bessi, H. Schwalbe, J. Dash, *Nucleic Acids Res.* **2018**, *46*, 5355–5365; b) P. C. Sharma, K. K. Bansal, A. Sharma, D. Sharma, A. Deep, *Eur. J. Med. Chem.* **2020**, *188*, 112016.
[20] X. Xie, B. Choi, E. Largy, R. Guillot, A. Granzhan, M. P. Teulade-Fichou, *Chem. Eur. J.* **2013**, *19*, 1214–1226.
[21] J.-L. Mergny, L. Lacroix, M.-P. Teulade-Fichou, C. Hounsou, L. Guittat, M. Hoarau, P. B. Arimondo, J.-P. Vigneron, J.-M. Lehn, J.-F. Riou, T. Garestier, C. Hélène, *Proc. Natl. Acad. Sci. USA* **2001**, *98*, 3062–3067.
[22] a) J. S. Hudson, L. Ding, V. Le, E. Lewis, D. Graves, *Biochemistry* **2014**, *53*, 3347–3356; b) J. Amato, B. Pagano, N. Borbone, G. Oliviero, V. Gabelica, E. D. Pauw, S. D'Errico, V. Piccialli, M. Varra, C. Giancola, *Bioconjugate Chem.* **2011**, *22*, 654–663; c) M. Bončina, Č. Podlipnik, I. Piantanida, J. Eilmes, M.-P. Teulade-Fichou, G. Vesnaver, J. Lah, *Nucleic Acids Res.* **2015**, *43*, 10376–10386.
[23] M. Di Antonio, A. Ponjavic, A. Radzevičius, R. T. Ranasinghe, M. Catalano, X. Zhang, J. Shen, L.-M. Needham, S. F. Lee, D. Klenerman, *Nat. Chem.* **2020**, *—12,* 832-837.
[24] a) P. Saha, D. Panda, R. Paul, J. Dash, *Org. Biomol. Chem.* **2021**, *19*, 1965–1969; b) M. Debnath, S. Ghosh, A. Chauhan, R. Paul, K. Bhattacharyya, J. Dash, *Chem. Sci.* **2017**, *8*, 7448–7456.
[25] a) D. Monchaud, C. Allain, M.-P. Teulade-Fichou, *Bioorg. Med. Chem.* **2006**,*16*, 4842; b) R. Paul, D. Dutta, R. Paul, J. Dash, *Angew. Chem. Int. Ed.* **2020**, *59*, 12507–12511; *Angew. Chem.* **2020**, *132*, 12407–12411.
[26] a) O. Domarco, C. Kieler, C. Pirker, C. Dinhof, B. Englinger, J. M. Reisecker, G. Timelthaler, M. D. García, C. Peinador, B. K. Keppler, *Angew. Chem. Int. Ed.* **2019**, *58*, 8007–8012; *Angew. Chem.* **2019**, *131*, 8091–8096; b) G. Biffi, D. Tannahill, J. McCafferty, S. Balasubramanian, *Nat. Chem.* **2013**, *5*, 182.
[27] L. Oh, *J. Biol. Chem.* **1951**, *193*, 265–266.

Manuscript received: March 11, 2021
Accepted manuscript online: April 14, 2021
Version of record online: ■■, ■■■

FULL PAPER

A pyridyl bis-thiazole, TPW preferentially binds to *c-KIT1* G-quadruplex over other G-quadruplexes and duplex DNA and emits high fluorescence inside cell nuclei. Despite being less toxic, it represses *c-KIT* transcription in cancer cells. These unique properties of **TPW** could be useful for the detection of G-quadruplexes and nuclear labeling of cancer cells.

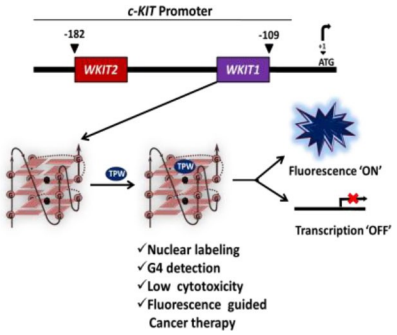

*R. Paul, Dr. D. Dutta, Dr. T. Das, Dr. M. Debnath, Prof. Dr. J. Dash**